

Temperature dependences of the parameters of atoms in the crystal structure of the intermediate-valence semiconductor SmB_6 : investigation by high-resolution powder neutron diffraction

This article has been downloaded from IOPscience. Please scroll down to see the full text article.

1993 J. Phys.: Condens. Matter 5 2479

(<http://iopscience.iop.org/0953-8984/5/16/007>)

View [the table of contents for this issue](#), or go to the [journal homepage](#) for more

Download details:

IP Address: 171.66.16.96

The article was downloaded on 11/05/2010 at 01:16

Please note that [terms and conditions apply](#).

Temperature dependences of the parameters of atoms in the crystal structure of the intermediate-valence semiconductor SmB_6 : investigation by high-resolution powder neutron diffraction

V A Trounov†, A L Malyshev†, D Yu Chernyshov†, M M Korsukova‡, V N Gurin‡, L A Aslanov§ and V V Chernyshev§

† Nuclear Physics Institute of the Russian Academy of Sciences, Gatchina 188350, Russia

‡ A F Ioffe Physical-Technical Institute of the Russian Academy of Sciences, St Petersburg 194021, Russia

§ Moscow State University, Moscow 119899, Russia

Received 28 January 1992, in final form 16 December 1992

Abstract. The crystal structure of intermediate-valence (IV) samarium hexaboride has been studied on single-crystal double-isotope samples $^{154}\text{Sm}^{11}\text{B}_6$ by x-ray diffractometry at room temperature and by high-resolution powder neutron diffraction in the temperature range $23\text{ K} \leq T \leq 300\text{ K}$. The x-ray experiment revealed the occurrence of vacancies at the boron site, larger thermal vibrations of the Sm atom than of La in the isostructural non-IV material LaB_6 and an aspherical charge distribution around the Sm nucleus. The neutron diffraction experiment confirmed the anomalous temperature dependence of the lattice parameter and revealed both a peculiar temperature dependence of the anisotropic thermal vibrations of the boron atom and a temperature-dependent change in the ratio of the isotropic thermal parameters of the Sm and B atoms. Thermal vibrations of the Sm ion can be satisfactorily described by the Einstein model with characteristic temperature $\Theta_E \approx 120\text{ K}$ within the whole temperature range. The data obtained are discussed in terms of the influence of the fluctuating valence of the Sm ion on the structural parameters of atoms.

1. Introduction

Samarium hexaboride SmB_6 , a well known typical intermediate-valence (IV) material characterized by an energy gap at the Fermi energy, like a semiconductor, has been the subject of intense experimental and theoretical studies for more than 25 years (see the reviews in [1–6]). The anomalies observed in the physical properties of SmB_6 are in any event related to the IV state of samarium ions. In particular, some anomalous features in the lattice dynamics of SmB_6 are explained by the interaction of phonons with valence fluctuations [6–8].

However, very little is known about the behaviour of the structural parameters of atoms in IV compounds. To our knowledge, there is only one single-crystal x-ray diffractometry study of $\text{Sm}_{0.7}\text{Y}_{0.3}\text{S}$ in which an anomalous temperature dependence of the Debye–Waller factor of sulphur atoms was reported and it was ascribed to the interaction of optic phonons with the fluctuating valence of Sm ions [9].

SmB_6 , like other rare-earth (RE) hexaborides, has a crystal structure with cubic symmetry (space group, $Pm\bar{3}m$ (O_h^1)) characterized by a three-dimensional skeleton of boron octahedra B_6 , the interstices of which are filled by the RE atoms [10].

High-precision x-ray diffraction studies on single crystals of LaB_6 and CeB_6 and their mixed crystals [11–14] revealed the occurrence of 2–6% of vacancies at the boron site as well as higher values of the temperature factors of RE atoms compared with those of the boron atoms which are 15 times lighter. For LaB_6 it has been shown that at room temperature the temperature factors of atoms mainly reflect the strength of interatomic forces, indicating a rigid boron framework and weaker boron–lanthanum bonding [15]. Contrary to these findings, about 20% of vacancies at the metal site and an extremely low value of the temperature factor of Sm atoms was recently reported for SmB_6 [12].

This ambiguity gave us the impetus to carry out systematic neutron diffraction studies of the crystal structure of RE hexaborides [16, 17] which confirmed the results of x-ray studies on LaB_6 , CeB_6 and their mixed crystals [11, 14]. In contrast with the results of [12] for SmB_6 , our combined neutron and x-ray diffraction studies utilizing the ‘zero-matrix’ technique [17] established the occurrence of about 4% of vacancies at the boron site and a considerably larger value for the temperature factor of Sm atoms than for that of boron atoms. The calculated value of the characteristic Einstein temperature $\Theta_E = 119.5$ K for Sm atoms [17] was in excellent agreement with the value $\Theta_E = 120$ K obtained by inelastic neutron scattering [18], testifying that the thermal parameters obtained are physically meaningful.

Another interesting result of these studies [11, 14, 16, 17] was the observation [17] that the values of mean square displacements of RE atoms systematically increase in the series $\text{LaB}_6 \rightarrow \text{CeB}_6 \rightarrow \text{SmB}_6$, i.e. the temperature factor of the Ce atom is 17% larger and that of the Sm atom is 28% larger than the temperature factor of the La atom although the lattice parameter in this series decreases by only 0.4% for CeB_6 and by 0.55% for SmB_6 . This increase in the temperature factor of RE atoms was assumed to be due to the enhanced interaction of lattice phonons with heavy electrons (CeB_6) or with valence fluctuations (SmB_6) [17].

The present investigation of the crystal structure of SmB_6 in the temperature range 23–300 K by high-resolution powder neutron diffraction was made with the aim of searching for the effects of the IV state (if any) on the structural parameters of atoms.

2. Experimental details

Double-isotope $^{154}\text{Sm}^{11}\text{B}_6$ single crystals were prepared by the high-temperature solution growth method [18] utilizing $^{154}\text{Sm}_2\text{O}_3$ and ^{11}B as the initial components. The purities of the starting materials were 95 mass%, 99 mass% and 99.9 mass% for amorphous boron, samarium oxide and Al, respectively. The degree of isotope enrichment was 99.3% for ^{11}B and more than 99% for ^{154}Sm . A detailed description of the preparation procedure can be found elsewhere [17]. A few isometric crystals were used for the single-crystal x-ray diffractometry study. Other crystals of mass about 10 g were ground into a fine powder and used in the neutron diffraction experiment.

For the x-ray diffraction experiment the isometric $^{154}\text{Sm}^{11}\text{B}_6$ crystal was ground to a sphere of 0.25 mm diameter. The integrated intensities of Bragg reflections were measured on a CAD-4 automated four-circle diffractometer using graphite-monochromated $\text{Mo K}\alpha$ radiation ($\lambda = 0.71069$ Å) at 298 K. An ω – 2θ continuous-scan technique was employed with a scan speed of 3° min^{-1} in ω . In total, 3143 reflections (190 independent) in

a hemisphere of the reciprocal space (index ranges $0 \leq h \leq 11$, $-11 \leq k \leq 11$, $-11 \leq l \leq 11$) were obtained. The intensities were corrected for Lorentz, polarization and absorption ($\mu R = 2.6$) effects. The equivalent reflections were averaged and used for structure refinements. The cell dimensions were determined by least-squares calculations based on 25 reflections ($62^\circ < \theta < 70^\circ$) obtained with Mo $K\alpha_1$ radiation ($\lambda = 0.70930 \text{ \AA}$).

The structure was refined by the full-matrix least-squares program AEI in a manner similar to that described in [17]. The variables refined were a scale factor k , the parameter x of the B atom, the thermal parameters (isotropic for the Sm atom and anisotropic for the B atom), the occupancy p of the boron site and the isotropic extinction parameter g . In the final refinement the possibility of anharmonic thermal vibrations for the Sm atom was tested (Gram-Charlier expansion up to the fourth-order tensor elements). Because of the high symmetry of the Sm position ($m\bar{3}m$), the non-zero anharmonic thermal parameters were $d_{1111} = d_{2222} = d_{3333}$ and $d_{1122} = d_{1133} = d_{2233}$. Residual electron densities were examined by calculating the deformation electron density maps (36 reflections with $\sin \theta / \lambda < 0.7 \text{ \AA}^{-1}$) for the (100) and (110) sections of the unit cell.

Neutron diffraction measurements were performed on the high-resolution powder diffractometer MINI-SFINKS utilizing the reverse Fourier time-of-flight method [19]. Neutron diffraction patterns of an approximately 2 cm^3 $^{154}\text{Sm}^{11}\text{B}_6$ powder sample filled in a cylindrical sample holder made of a titanium-zirconium alloy were recorded at nine temperatures in the temperature range 23–300 K, using an RG210 Leybold-Heraeus refrigerator. The temperature stability during the measurements was kept to within 3 K; the temperature gradient for a sample of about 3 cm height was less than 0.5 K cm^{-1} . The counting time at each temperature was 10 h.

The data obtained were analysed by a modified Rietveld method [20], employing the values of the scattering lengths given in [21] and allowing for the degree of isotope enrichment of ^{11}B . The integrated intensities were corrected for the absorption [22] and primary extinction effects [23]. The variables refined were the lattice parameter, the parameter x of the B atom, the thermal parameters (isotropic for the Sm atom and anisotropic for the B atom), two peak half-width parameters, a scale factor, six 'background parameters' (coefficients of the polynomial background description [20]) and the effective size of the mosaic block. Because of the large correlations between some of the parameters (e.g. the occupancy of the boron site and the temperature factors of boron), they were refined separately. Full structure refinements were made for each data set in the temperature range studied.

3. X-ray diffraction results

The results of the structure refinements assuming harmonic and anharmonic thermal vibrations of the Sm atom are presented in table 1. In general, the data presented are in excellent agreement with our previous results for the 'zero-matrix' $^{152}\text{Sm}_{0.615}^{154}\text{Sm}_{0.385}^{11}\text{B}_6$ sample [17], i.e. they confirm the occurrence of vacancies at the boron site and the larger temperature factor of the Sm atom compared with that of the B atom (see section 1). It can also be seen that the parameters for anharmonic contributions to the thermal vibrations of the Sm ion are very small and can in practice be neglected. Thus, the restoring potential around the Sm ion is essentially harmonic, and the observed increase in the Sm temperature factor in SmB_6 compared with that of La in LaB_6 cannot be explained by anharmonicity effects.

Table 1. Final structure data and refinement characteristics for the single-crystal $^{154}\text{Sm}^{11}\text{B}_6$ (space group $Pm\bar{3}m$ (No. 221); Sm in 1a and B in 6f). The standard deviations are given in parentheses. The cell dimensions are $a = b = c = 4.1332(2)$ Å.

	All data, Sm harmonic	All data, Sm anharmonic
Boron		
Occupancy p_B	0.97(1)	0.97(1)
Fractional coordinate x_B	0.199 8(3)	0.199 6(3)
U_{11} (Å ²)	0.002 95(39)	0.002 66(34)
U_{22} (Å ²)	0.004 74(31)	0.004 45(27)
Samarium		
U_{330} (Å ²)	0.006 95(4)	0.005 86(14)
$d_{111}(\times 10^8)$		-12(2)
$d_{112}(\times 10^8)$		-5.1(1)
Extinction parameter g	0.205(8)	0.160(8)
Agreement factors		
R	0.0111	0.0074
R_w	0.0125	0.0090
Goodness of fit S	0.5	0.3

The deformation electron density maps for the (110) and (100) sections of the unit cell from both harmonic and anharmonic refinements manifest positive peaks of 1.3(3) electrons Å⁻³ in the (100) direction, 0.75 Å distant from the Sm nucleus, and negative peaks of -1.2(1.2) electrons Å⁻³ in the (111) direction. Qualitatively, the picture is very similar to the aspherical charge distribution around the Ce nucleus in CeB₆ [13, 14], although the negative peaks around the Sm nucleus are within the error limit. In the case of CeB₆ it was assumed that the charge asphericity reflects the crystal-field splitting of the 4f¹ state of the Ce³⁺ ions into a Γ_8 quartet (ground state) and Γ_7 doublet (about 530 K higher), so that the positive peaks indicate the excess electron population in Γ_8 and the negative peaks indicate the electron population deficiency in Γ_7 [13]. For SmB₆ it was suggested that the ground state of the crystal-field-split $J = \frac{5}{2}$ level of the Sm ion is a Γ_8 quartet, with a Γ_7 doublet lying at a higher energy level [2]. Therefore, the positive peaks at present observed around the Sm nucleus may reflect the level splitting and the presence of the Γ_8 ground state for the Sm ion.

4. Neutron diffraction results

Figure 1 shows an example of the experimental neutron diffraction spectrum of the $^{154}\text{Sm}^{11}\text{B}_6$ sample at 300 K. The structure data obtained from the profile refinements are presented in table 2. A comparison with the x-ray data for room temperature (table 1) shows the close agreement between the values of the structural parameters. The only discrepancy exceeding two standard deviations is that between the boron site occupancies, and even here the difference is about 5%. This consistency gives more confidence in the powder neutron values in the whole temperature range studied and provides a firmer background for discussing their variation with temperature.

The lattice parameter value of our $^{154}\text{Sm}^{11}\text{B}_6$ sample at room temperature is in fairly good agreement with the values reported in the literature for the stoichiometric samples ($a = 4.1334(2)$ Å [24], $a = 4.1326(1)$ Å [7], $a = 4.1339(1)$ Å [8] and $a = 4.1342(5)$ Å

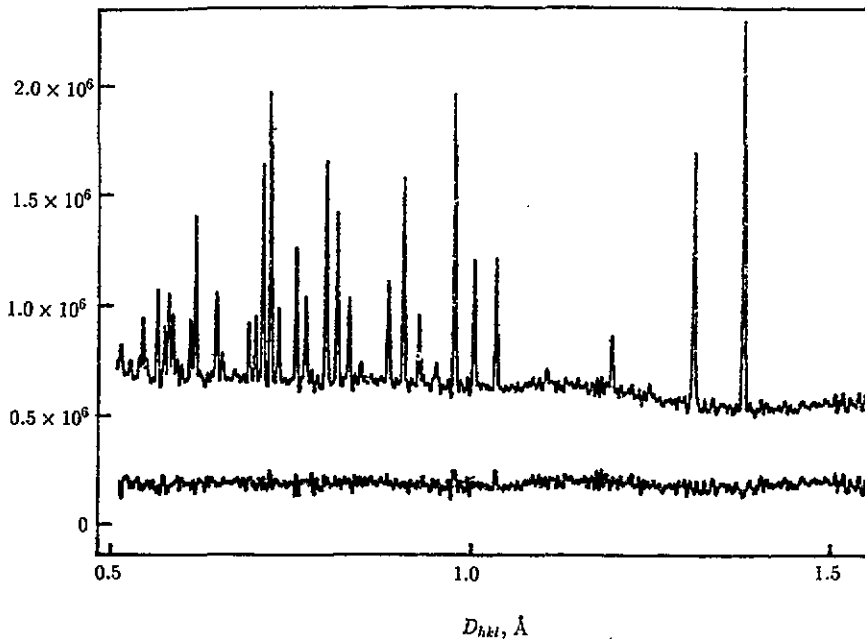


Figure 1. Neutron diffraction pattern of $^{154}\text{Sm}^{11}\text{B}_6$ at 300 K. The lower curve represents the difference between the observed and calculated profiles.

Table 2. Final structure data and refinement characteristics for $^{154}\text{Sm}^{11}\text{B}_6$ at different temperatures from high-resolution powder neutron diffraction. The standard deviations are given in parentheses.

	$T = 300 \text{ K}$	$T = 153 \text{ K}$	$T = 23 \text{ K}$
Lattice parameter a (\AA)	4.133 19(3)	4.131 73(3)	4.133 02(3)
Boron			
Occupancy p_{B} (%)	91.5(5)	91.5(5)	91.5(5)
Fractional coordinate x_{B}	0.199 73(7)	0.199 64(7)	0.199 77(6)
U_{11} (\AA^2)	0.002 45(14)	0.002 51(12)	0.001 16(12)
U_{22} (\AA^2)	0.004 83(10)	0.004 16(9)	0.003 35(9)
Samarium			
U_{iso} (\AA^2)	0.006 74(14)	0.004 20(12)	0.001 39(12)
Extinction parameter R (μm)	1.48(9)	1.48(9)	1.48(9)
Goodness of fit S^2	4.5	3.1	4.08

[25]). The temperature dependence of the lattice parameter as presented in figure 2 is qualitatively the same as measured earlier by the x-ray diffraction technique [7, 25]: it goes through a smooth minimum near 150 K. This anomalous behaviour has been explained by a change in the electronic configuration of the samarium ion with decreasing temperature [25]. It has thus been inferred that between 300 and 4 K the average Sm valency changes from 2.60 to 2.53, corresponding to an increase of 17.5% of Sm^{2+} ions.

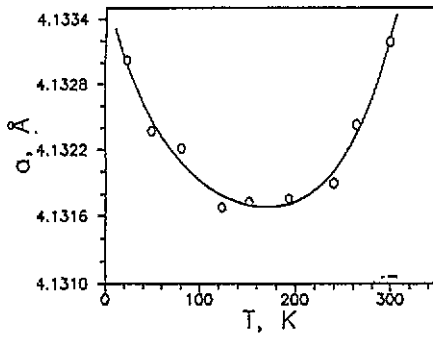


Figure 2. Temperature dependence of the lattice parameter of $^{154}\text{Sm}^{11}\text{B}_6$: —, fit of the experimental points with a polynomial of $n = 4$ degree.

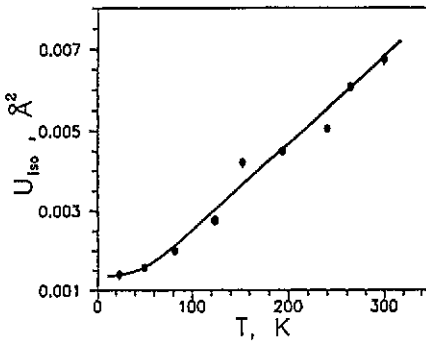


Figure 3. Temperature dependence of the isotropic thermal parameter of the Sm atom: —, curve calculated for Sm in the Einstein model with $\Theta_E = 120$ K.

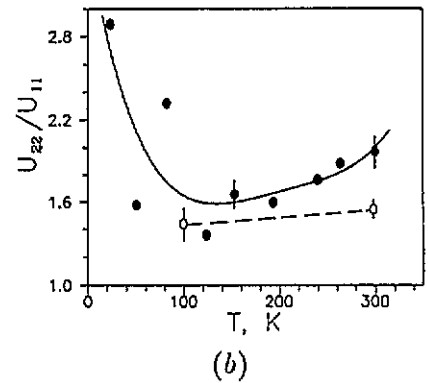
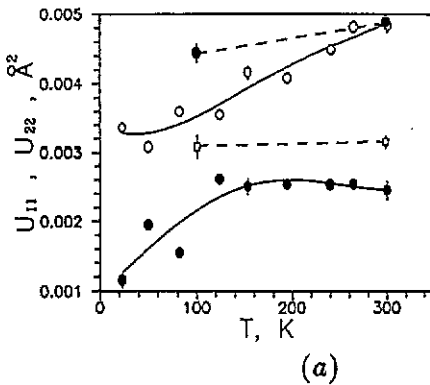


Figure 4. (a) The variation with temperature in the anisotropic thermal parameters of the boron atom in $^{154}\text{Sm}^{11}\text{B}_6$: ●, U_{11} ; ○, U_{22} . The corresponding parameters U_{11} (□) and U_{22} (●) for the boron atom in CeB_6 [13] are shown for comparison. (b) The temperature dependence of the ratio U_{22}/U_{11} for SmB_6 (●) and for CeB_6 (○): —, fit of the experimental points with a polynomial of $n = 4$ degree.

The temperature dependences of the thermal parameters of atoms in SmB_6 are presented in figures 3–5.

Lattice dynamics studies of SmB_6 [8] and some other RE hexaborides [26–28] at

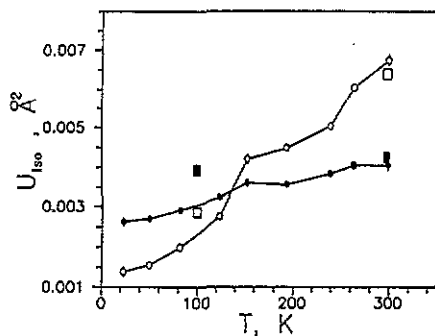


Figure 5. Temperature dependence of the isotropic thermal parameters of atoms in SmB_6 (\circ , Sm; \bullet , B). The corresponding values for Ce (\square) and B (\blacksquare) in CeB_6 at $T = 100$ K and $T = 298$ K are taken from [13].

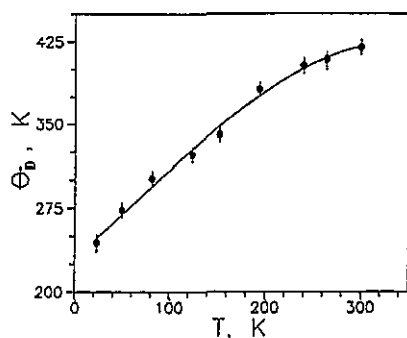


Figure 6. Temperature dependence of the effective Debye temperature for the boron sublattice of $^{154}\text{Sm}^{11}\text{B}_6$ (the Θ_D values were calculated from the thermal parameters using the standard formula [29] and assuming that a boron octahedron can be approximated by one atom only of atomic weight $6m_B$): —, fit of the experimental points with a polynomial of $n = 4$ degree.

room temperature revealed the non-interacting vibrations of the RE atoms which can be described by the Einstein model with a characteristic Einstein temperature Θ_E . Therefore, we calculated the Θ_E -values from the values of the isotropic thermal parameter of the Sm atom presented in figure 3, using the formula given in [29]. These values remain nearly constant in the whole temperature range; the mean value of Θ_E is about 120 K. The temperature dependence of the temperature factor of the Sm atom calculated in the Einstein model with $\Theta_E = 120$ K is shown in figure 3 by the full curve. Quite satisfactory agreement between the experimental and calculated values confirms the assumed weak interaction between the boron and the metal sublattices and within the metal sublattice in SmB_6 in the whole temperature range.

In other words, the variation in the mean square amplitude of thermal vibrations of the Sm ion with temperature is absolutely normal, demonstrating that, within the accuracy of the present experiments, the thermal vibrations of Sm remain unaffected by the valence change of the Sm ion with decreasing temperature [25]. A similar normal temperature behaviour was observed for the metal temperature factor in the IV compound $\text{Sm}_{0.7}\text{Y}_{0.3}\text{S}$ [9].

However, at room temperature, the $\langle u^2 \rangle$ -value of Sm in SmB_6 is about 25% larger than the $\langle u^2 \rangle$ -value of La in LaB_6 as determined in [11]. The room-temperature phonon spectra of LaB_6 [27] and SmB_6 [8] showed unusually flat acoustic modes. The explanation given there and confirmed by the present data is that the RE ions behave as Einstein oscillators. Comparing the Einstein frequencies ω_E in LaB_6 [27] and in SmB_6 [8], one can see that $\omega_E(\text{La})$ is at least 14% higher than $\omega_E(\text{Sm})$. Since $\langle u^2 \rangle$ is proportional to T/ω_E^2 at elevated temperatures, the observed difference between the mean square amplitudes of La and Sm

corresponds to the difference in Einstein frequencies.

The overall softening of the vibrational spectrum of SmB_6 in comparison with that of LaB_6 was observed in [8] and this softening was attributed to the effects of the fluctuating valence of the Sm ion. However, since there seems to be a systematic increase in $\langle u^2 \rangle$ for RE ions in the series $\text{LaB}_6 \rightarrow \text{CeB}_6 \rightarrow \text{SmB}_6$ [17], one should conclude that the reasons for the large difference between the Einstein temperatures of La and Sm remain an open question.

The temperature dependences of the anisotropic thermal parameters of the boron atom as presented in figure 4(a) are relatively weak as one should expect from the rigidity of the boron framework. However, note that the U_{11} -value remains nearly constant in the temperature range 300–120 K and decreases rapidly below 120 K, while U_{22} smoothly decreases in the whole temperature range.

The anisotropy of the thermal vibrations of the boron atom, $U_{22} > U_{11}$, reflects the peculiar chemical bonding in the boron sublattice of the hexaboride structure where inter-octahedral B–B bonds are shorter (and stronger) than the intra-octahedral B–B bonds (see [11], and references therein). The parameter U_{11} represents the vibrations of the B atom in the direction of the inter-octahedral bond, while the parameters $U_{22} = U_{33}$ represent vibrations in the directions normal to this bond. In this sense the boron sublattice is a rigid framework made up of 'loose' boron octahedra. Thus the value of the ratio U_{22}/U_{11} can be used to characterize the 'loosening' of the boron octahedron. The temperature dependence of this ratio is shown in figure 4(b). One can see a flat minimum at 150 K and a noticeable increase when the temperature decreases to 23 K. The value of U_{22}/U_{11} at 23 K is about 40% higher than that at 300 K. There is a striking similarity between the temperature dependence of the ratio U_{22}/U_{11} for the boron atom in SmB_6 and that of the isotropic thermal parameter U_S of the sulphur atom in the IV $\text{Sm}_{0.7}\text{Y}_{0.3}\text{S}$ observed in [9]. The anomaly in $U_S(T)$ was supposed to indicate a softening of optic phonons caused by the fluctuating valency of the Sm ion [9].

It is very tempting to propose a similar explanation for the case of SmB_6 . Indeed, a softening of optic phonons in the SmB_6 spectrum compared with that of LaB_6 was observed [8]. However, the relation between the individual temperature factors of the boron atom and the phonon frequencies in SmB_6 is not as straightforward as in the case of the Sm ion. The occurrence of boron vacancies further complicates the interpretation of the results. A more sophisticated model should be developed to distinguish between the effects of the different phenomena.

As mentioned above (see section 1), at room temperature in the crystal structure of the RE hexaborides the thermal vibrations of boron are smaller than those of the RE metal. Figure 5 shows the temperature dependences of the isotropic temperature factors of Sm and B atoms (the latter was calculated from anisotropic refinements). It can be seen that, at temperatures higher than $T \simeq 150$ K, $U_{\text{iso}}(\text{Sm}) > U_{\text{iso}}(\text{B})$ while, at $T < 150$ K, the thermal vibrations of boron became larger than those of Sm. From the data presented in [13], one can see that a similar relation is observed in CeB_6 : $U_{\text{iso}}(\text{Ce}) > U_{\text{iso}}(\text{B})$ at $T = 300$ K and $U_{\text{iso}}(\text{Ce}) < U_{\text{iso}}(\text{B})$ at $T \approx 100$ K. This behaviour may be evidence of a general softening of the boron sublattice with decreasing temperature. This assumption seems to be supported by the data presented in figure 6. One can see that the effective Debye temperature of the boron sublattice is nearly constant in the temperature range 300–200 K and rapidly decreases below 200 K with decreasing temperature. The same seems to be true for CeB_6 ; the value of Θ_D at 300 K is considerably higher than at 100 K (as calculated by us from the data presented in [13]). Since CeB_6 is an abnormal compound (dense Kondo system), more systematic studies on the crystal structures of other hexaborides, and also 'normal' LaB_6 ,

within a broader temperature range are necessary to decide whether this peculiar behaviour is an intrinsic property of the crystal structure itself or arises for other reasons.

5. Conclusions

To summarize, we wish to point out those results of the present study which may be regarded as a manifestation of the intermediate-valence state of the Sm ion in SmB₆:

- (i) the temperature dependence of the lattice parameter;
- (ii) the aspherical charge distribution around the Sm nucleus;
- (iii) the decrease in the Einstein temperature for Sm in comparison with that of La;
- (iv) the peculiar temperature dependence of the ratio U_{22}/U_{11} of the anisotropic thermal parameters of the boron atom.

These results are in accord with the data on the physical properties of SmB₆ accumulated so far.

References

- [1] Vainstein E E, Blokhin S M and Paderno Yu B 1964 *Sov. Phys.—Solid State* **6** 2909
- [2] Kasuya T, Kojima K and Kasaya M 1977 *Valence Instabilities and Related Narrow Band Phenomena* ed R D Parks (New York: Plenum) pp 137–52
- [3] Kasuya T, Takegahara K, Fujita T, Tanaka T and Bannai E 1979 *J. Physique* **40** C5 308
- [4] Mott N F 1982 *Valence Instabilities* ed P Wachter and H Boppart (Amsterdam: North-Holland) pp 403–20
- [5] Kasuya T, Kasaya M, Takegahara K, Fujita T, Goto T, Tamaki A, Takigawa M and Yasuoka H 1983 *J. Magn. Magn. Mater.* **31–4** 447
- [6] Wachter P 1987 *Proc. 10th Int. Symp. on Boron, Borides and Related Compounds* (Duisburg: Duisburg University) pp 166–75
- [7] Alekseev P A, Konovalova E S, Lazukov V N, Lukshina S N, Paderno Yu B, Sadikov I P and Gorvenko E V 1988 *Sov. Phys.—Solid State* **30** 2024
- [8] Alekseev P A, Ivanov A S, Dorner B, Schober H, Kikoin K A, Mishchenko A S, Lazukov V N, Konovalova E S, Paderno Yu B, Rumyantsev A Yu and Sadikov I P 1989 *Europhys. Lett.* **10** 457
- [9] Demier P, Weber W and Longinotti L D 1976 *Phys. Rev. B* **14** 3635
- [10] Von Stackelberg M and Neumann F 1932 *Z. Phys. Chem.* **19** 314
- [11] Korsukova M M, Lundström T, Gurin V N and Tergenius L-E 1984 *Z. Kristallogr.* **168** 299
- [12] Eliseev A A, Efremov V A, Kuzmicheva G M, Konovalova E S, Lazorenko V I, Paderno Yu B and Khlyustova S Yu 1986 *Sov. Phys.—Crystallogr.* **31** 476
- [13] Sato S 1985 *J. Magn. Magn. Mater.* **52** 310
- [14] Blomberg M K, Merisalo M J, Korsukova M M and Gurin V N 1989 *J. Less-Common Met.* **146** 309; 1991 *J. Less-Common Met.* **168** 313
- [15] Korsukova M M, Lundström T, Tergenius L-E and Gurin V N 1987 *Solid State Commun.* **63** 187
- [16] Trunov V A, Malyshev A L, Chernyshev D Yu, Kurbakov A I, Korsukova M M and Gurin V N 1991 *J. Appl. Crystallogr.* **24** 142
- [17] Trunov V A, Malyshev A L, Chernyshev D Yu, Korsukova M M, Gurin V N, Aslanov L A and Chernyshev V V 1991 *J. Appl. Crystallogr.* **24** 888
- [18] Korsukova M M, Stepanov N N, Gontcharova E V, Gurin V N, Nikanorov S P and Smirnov I A 1981 *J. Less-Common Met.* **82** 211
- [19] Antson O, Bulkin A P, Hiismaki P E, Korotkova T K, Kudryashev V A, Kukkonen H S, Muratov V G, Poyry H O, Shchebetov A F, Tiitta A T, Trunov V A and Ul'yanov V A 1989 *Physica B* **156–7** 567
- [20] Zlokazov V B and Chernyshev V V 1992 *J. Appl. Crystallogr.* **25** 447
- [21] Sears F 1984 *Chalk River Nuclear Laboratories, Atomic Energy of Canada Ltd. Report AECL-8490*
- [22] Rouse K D, Cooper M J, York E J and Chakera A 1970 *Acta Crystallogr. A* **30** 682

- [23] Becker P and Coppens P 1974 *Acta Crystallogr. A* **30** 129
- [24] Paderno Yu B and Lundström T 1983 *Acta Chem. Scand. A* **37** 609
- [25] Tarascon J M, Isikawa Y, Chevalier B, Etourneau J, Hagenmuller P and Kasaya M 1980 *J. Physique* **41** 1141
- [26] Shell G, Winter H, Reitschell H and Gompf F 1982 *Phys. Rev. B* **25** 1589
- [27] Smith H G, Dolling G, Kunii S, Kasaya M, Goto T, Lui B, Takegahara K and Kasuya T 1985 *Solid State Commun.* **53** 15
- [28] Peysson Y, Daudin B, Dubus M and Benenson R E 1986 *Phys. Rev. B* **34** 8367
- [29] Willis B T M and Pryor A W 1975 *Thermal Vibrations in Crystallography* (Cambridge: Cambridge University Press)